

MARIUSZ BANASZKIEWICZ*

Numerical investigation of creep behaviour of high-temperature steam turbine components

ALSTOM Power Ltd., Stoczniowa 2, 82-300 Elbląg, Poland

Abstract

The paper presents a model for creep basing on the so-called characteristic creep strain. It illustrates its application in computations of old steam turbines components. The presented model is a modification of the Norton model which relates the stress exponent to the creep rupture strength and current stress. Creep strain is a function of the above two quantities, i.e., rupture strength and current stress, and a characteristic creep strain which is material constant for a given time and temperature. Computational examples regard the rotating and pressure components analysed using the finite element method.

Keywords: Creep; Lifetime assessment; Steam turbine

Nomenclature

- n – constant stress exponent
- m – exponent in the power-law relationship
- t – time, h
- T – temperature, °C

Greek symbols

- ε – strain
- ε_C – creep strain
- ε_D – datum strain
- ε_χ – characteristic creep strain
- σ – stress, MPa
- σ_R – creep rupture strength, MPa

*E-mail address: mariusz.banaszkiewicz@power.alstom.com

1 Introduction

Creep is a major damage mechanism limiting the useful life of high-temperature (above 400 °C) steam turbine components. The essence of creep consists in slow and continuous material deformation under constant load which is brought about by thermal activation at high temperatures [1]. Accumulation of irreversible creep strains may lead to unacceptable large changes in dimensions or geometrical deformations, and in extreme cases can cause material damage by rupture. Depending on the component, the final damage can be controlled by deformation or rupture [2].

In high power output steam turbines operating at inlet temperatures above 535 °C and being in service for over 200 000 h, creep strains are important for two basic reasons [3]:

- Small creep strains are important as rotors, casings and diaphragms deformations lead to clearance reduction, or in case of bolts and shrink rings to the loss of tension. In this case, the level of strain is in the range 0.03–0.15%,
- Accumulation of larger creep strains is important in remaining lifetime assessments of rotors, casings and valve chests both in relation to the general level of strain and to the local strains at stress concentration areas. The level of creep strains of interest is in this case 1–5%.

Due to the importance of both small and high creep strains, it is desired to have an accurate description of creep strain accumulation over time in quite a broad range of strain values. In engineering calculations the Norton creep model [4,5] is most frequently used and it describes the creep strain rate as a function of stress raised to a constant exponent. In reality, for creep resistant steels this exponent is highly variable depending on the strain level, and the validity of the Norton model is limited to steady-state creep (secondary creep regime) and to a narrow range of creep strains. Making the power exponent in the Norton model a function of stress and creep rupture stress leads to a more accurate description of creep validated by experimental investigations.

The paper describes a mathematical model of creep developed at ALSTOM and presents results of numerical calculations carried out for steam turbine components designed according to creep criteria. The objective of these calculations is to investigate the usefulness of this model in predicting creep life of old steam turbines designed in sixties and seventies by the company Zamech, taking into account their specific design features and available material data. The turbines were designed using simple analytical solutions for stresses which were then assessed based on the creep rupture properties and required safety factors. Using modern computational techniques and new constitutive models in assessing creep

life of old turbines requires prior detailed investigations proving the reliability and acceptability of calculation results.

2 Characteristic creep strain model

According to the Norton law the relationship between creep strain, ε_C , and constant stress, σ , at a given temperature, T , and time, t , is described by exponential function of stress, based on which the stress exponent can be written as

$$\frac{\partial \log \varepsilon_C}{\partial \log \sigma} = n = \text{const} . \quad (1)$$

Experimental creep curves plotted in $\log \varepsilon_C - \log \sigma$ system show that the inclination angle is not constant, $n \neq \text{const}$, and at small strains and stresses are close to unity, while at high strains, when stresses are near the creep rupture strength, the exponent n goes to infinity. Bolton, based on the analyses of creep tests results, proposed the following isochronous relation between the stress exponent and stress expressed as a fraction of creep rupture strength [3,6]

$$\frac{\partial \log \varepsilon_C}{\partial \log \sigma} = n = \frac{1}{1 - \frac{\sigma}{\sigma_R}} , \quad (2)$$

where σ_R denotes the creep rupture strength for a given time and at constant temperature. Integrating the above relationship, one obtains the equation for creep strain in the form

$$\varepsilon_C = \frac{\varepsilon_\chi}{\frac{\sigma_R}{\sigma} - 1} \quad (3)$$

where ε_χ is the characteristic creep strain being a material constant at a given time and temperature. For a constant characteristic creep strain, the model can be augmented by power relationship between rupture strength and time

$$\sigma_R \propto t^{\frac{-1}{m}} ; \quad (4)$$

where m denotes exponent in the power-law relationship.

The creep model described by Eqs. (3) and (4) must be closed by the following three constants:

1. σ_{R1} – creep rupture strength at time t_1 ,
2. σ_{R2} – creep rupture strength at time t_2 ,
3. σ_{D1} – creep strain, ε_D stress at time t_1 .

Expressing Eq. (3) by the above three constants we obtain

$$\varepsilon_C = \frac{\varepsilon_D \left(\frac{\sigma_{R1}}{\sigma_{D1}} - 1 \right)}{\frac{\sigma_R}{\sigma} - 1}. \quad (5)$$

Taking into account function (4), the creep rupture strength can be written in the form

$$\sigma_R = \sigma_{R1} \left(\frac{t_1}{t} \right)^{1/m}, \quad (6)$$

where

$$m = \frac{\log \left(\frac{t_2}{t_1} \right)}{\log \left(\frac{\sigma_{R1}}{\sigma_{R2}} \right)}. \quad (7)$$

Finally, combining Eq. (5) with (6) the model relationship between creep strain and time at constant stress assumes the form

$$\varepsilon_C = \frac{\varepsilon_D \left(\frac{\sigma_{R1}}{\sigma_{D1}} - 1 \right)}{\frac{\sigma_{R1}}{\sigma} \left(\frac{t_1}{t} \right)^{1/m} - 1}. \quad (8)$$

Creep curves for a 1%CrMoV steel at temperature 500 °C calculated using Eq. (9) for three different stress values 235, 250 and 260 MPa are shown in Fig. 1. The curves clearly reproduce the experimentally measured creep curves of steels with clearly visible primary, secondary and tertiary creep periods, whose duration, according to plot and in line with creep tests [3], depends on the stress level. These facts confirm physical correctness of the presented mathematical model of the creep based on characteristic creep strain.

3 Computation results of creep finite element analysis

3.1 Creep of valve casings

Creep calculations are normally performed at turbine design phase and after 100 000 service hours in the framework of damage and residual lifetime assessment of turbine main components. Valves casings are among the most highly loaded components of steam turbines. High parameters of steam, both pressures and temperatures, cause that valve casings are particularly exposed to creep damage.

200 MW steam turbines are the most numerous machines in the Polish power generation industry and so far the results of simplified 2D calculations using the Norton model were available for this turbine [5]. This work is a first attempt to

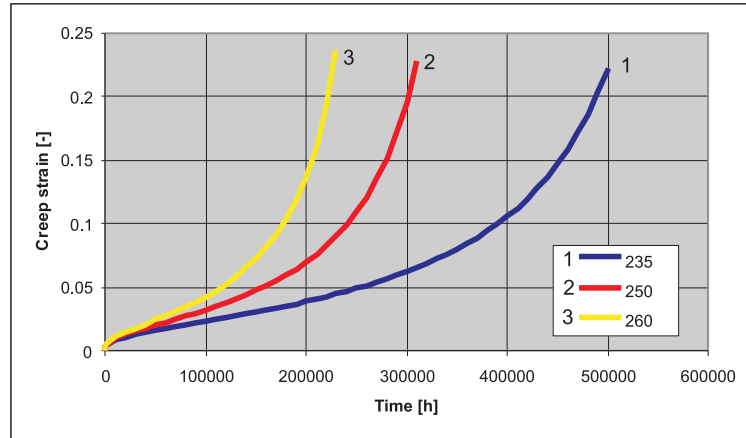


Figure 1. Primary creep curves at constant stress calculated using characteristic creep strain model.

analyse the creep behaviour of high-pressure stop valve casing of this machine using 3D geometry model and material specific creep properties. Computations were carried out using ABAQUS code [7], basing on the finite element method [8], and employing the user subroutine called *creep*. The characteristic creep strain model was implemented in this subroutine and configured with the appropriate material data describing creep behaviour of the valve casing cast steel L17HMF. Constant casing metal temperature and steam pressure were assumed in calculations. As it is seen from Fig. 2a presenting the Huber-Mises elastic stress distribution, the stress distribution within the casing in elastic condition is very nonuniform. Maximum stress occurs at the swirl braker in the inlet chamber, where equivalent stress reaches 260 MPa in a very confined area. This is a location where cracking was found by non-destructive testing of valve casings carried out during major overhauls. Stress concentrations also occur in the transition areas between pipelines and cylindrical (inlet) and spherical (outlet) regions of the valve casing. These areas are not possible to be correctly modelled in two-dimensional computations and only 3D approach enables identification of all critical locations where crack initiation can be expected. The stress level in the latter two regions is much lower – approx. 120 MPa – but occurs on bigger areas. After 150 000 service hours in creep the stress distribution in the casing is more uniform (Fig. 2b) and far lower peak stresses at stress concentration locations exist. Equivalent stresses in both locations analysed are practically equal and do not exceed 70 MPa. Despite stress relaxation and redistribution, creep strains after 150 000 h (Fig. 3), are significantly different, what results from the initially different elastic stresses.

Figure 4 presents stress and strain evolution in the whirl braker area and outlet section of the valve casing. According to the presented creep model and

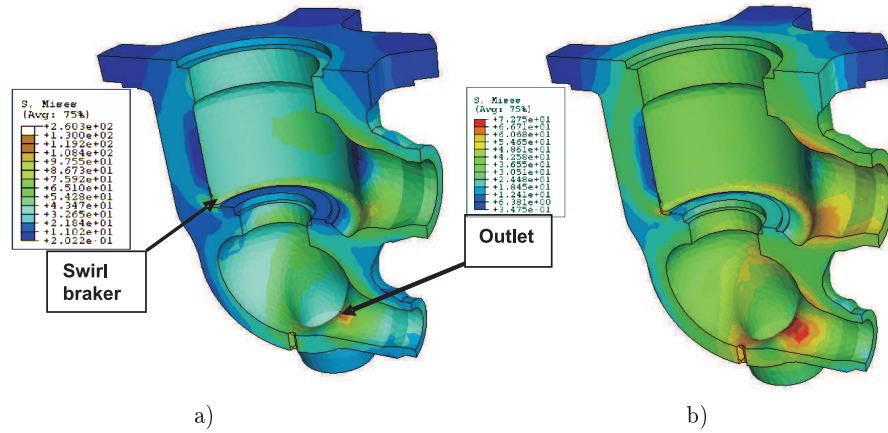


Figure 2. Huber-Mises stress distribution in elastic condition (a) and creep condition after 150 000 h (b).

in line with experimentally observed behaviour of steels at high temperatures, in the initial operation time fast stress relaxation occurs, but its rate decreases over time and practically vanishes after some dozen of thousands of service hours relaxation. The primary and secondary creep periods are clearly seen on the creep curves describing the creep strain accumulation, where strain accumulation rate decreases over time in the primary creep region and reaches a constant value in the secondary creep regime.

3.2 Creep of rotors

The same creep model was used to analyse the creep behaviour of a steam turbine rotor. Although a variety of creep models are available for steam turbine components [9], the advantage of the characteristic strain model is the use of material and temperature dependent creep data which are available not only for new steels but also for older material types.

Creep of rotors takes place at nonuniform temperature and stress fields. It is illustrated in Fig. 5. presenting temperature distribution within high-pressure rotor of a 55 MW Zamech turbine, and in Fig. 6 presenting the Huber-Mises stress distributions in elastic condition and in creep conditions after 200 000 service hours. Temperature distribution in the rotor is determined by the expanding steam temperature and heat transfer coefficients, mainly in the rotor glands. Highest temperatures and therefore fastest creep rates occur in the inlet sections of the rotor, in the region of control stage which is also most highly efforted due to stresses resulting from centrifugal forces. Generally, three locations of highest creep damage can be identified in the region of high-pressure control stage:

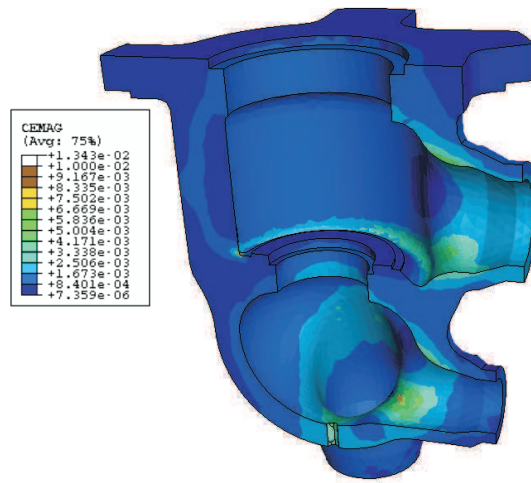


Figure 3. Creep strain distribution after 150 000 h.

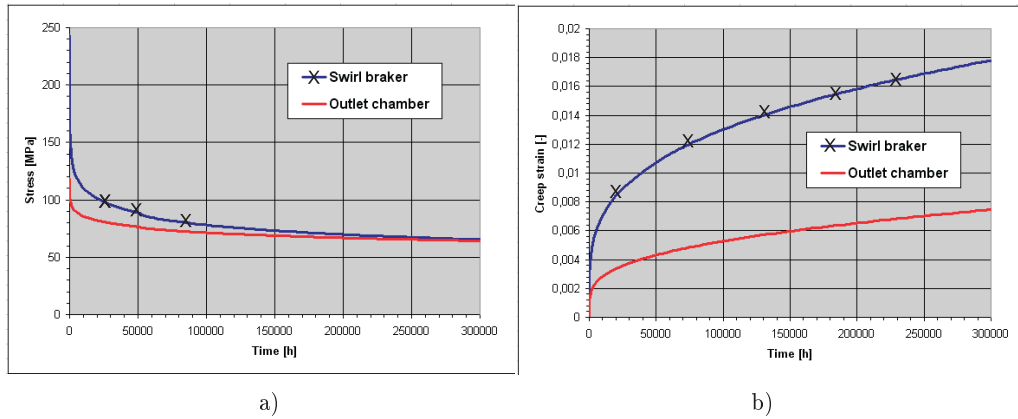


Figure 4. Huber-Mises stress relaxation (a), and creep strain accumulation (b) in the most highly efforted areas of valve casing.

- disc-to-shaft transition on the left-hand side of the disc,
- disc-to-shaft transition on the right-hand side of the disc,
- rotor bore surface underneath the control stage disc.

Disc elastic stresses reach 120 MPa, while in the rotor bore they are on the level of 90 MPa. In the analyzed regions, the highest temperature prevails on the right-hand side of the control stage disc. After 200 000 service hours in creep, the control stage stresses become more uniform and their maximum does not exceed 90 MPa.

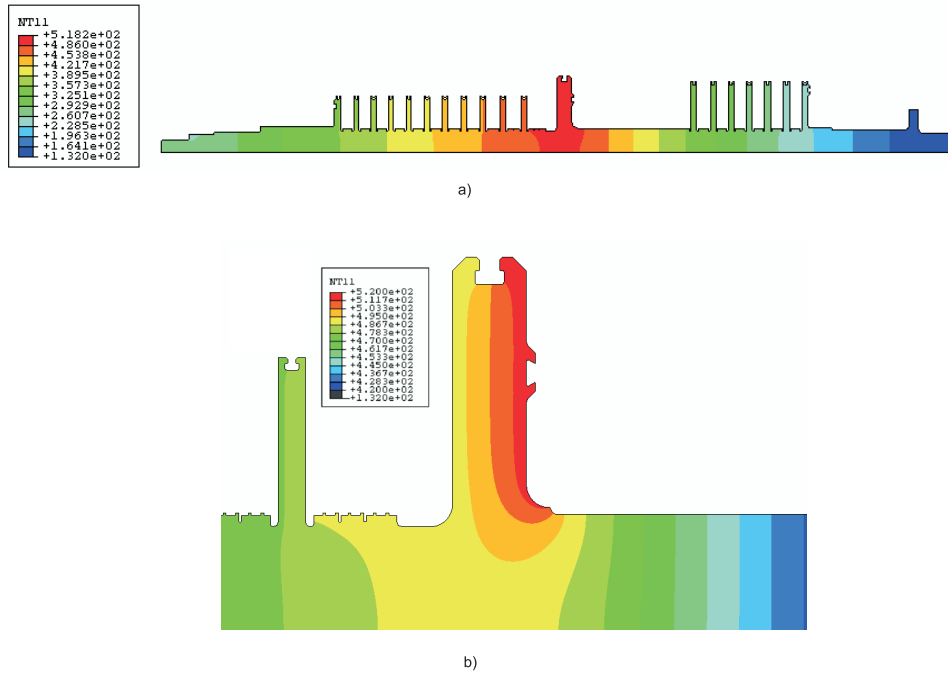


Figure 5. Temperature distribution in the rotor (a), and in control stage region (b).

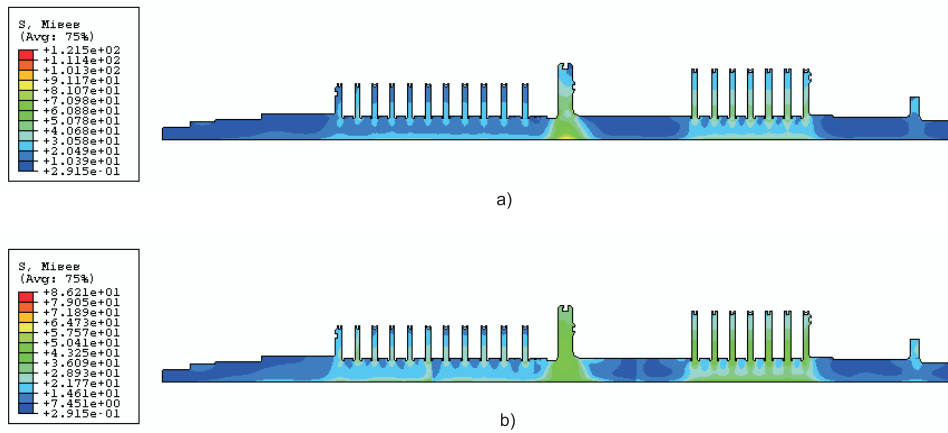


Figure 6. Huber-Mises equivalent stress distribution in elastic (a) and creep conditions after 200 000 service hours (b).

The above mentioned critical areas exhibit at the same time the highest rate of creep strain accumulation, whose distribution is shown in Fig. 7. On the transition radius from the disc to shaft, maximum creep strains exceed 0.7% and are highly concentrated. The areas with creep strains of 0.5% are much larger and occur,

among others, on the rotor bore surface. The level of creep strains after 200 000 service hours is below the generally acceptable value of 1%. This fact confirms the useful life of the rotor in excess of 200 000 hours and is in agreement with design lifetime calculations and field experience.

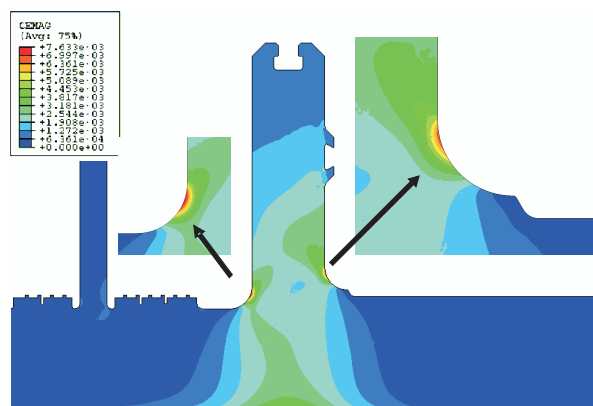


Figure 7. Creep strain distribution in the control stage area after 200 000 service hours.

Stress relaxation and creep strain accumulation processes presented in Fig. 8 indicate that the location of maximum stress and maximum strain regions varies over time and the locations of highest stresses do not correspond to the locations of currently largest creep strains. Hence, creep life assessment of rotors carried out on the basis of the condition of area with highest elastic stress is not necessarily fully reliable, and the area of largest creep strain does not always correspond to the area of highest elastic or creep stress. As described in [10] the creep ductility is a very important measure of creep life exhaustion, in particular at high stress concentration areas, like those present in turbine rotors. Only full analysis of the state of stress and strain during rotor operation in long period of time provides a basis for reliable calculation of the creep damage and remaining lifetime predictions of steam turbine rotors.

4 Summary

The presented results of finite element calculations of turbine components creep are based on the mathematical model which is an extension of the Norton model into unsteady creep regions (primary and tertiary creep). Simple and accurate enough, from the engineering point of view, description of all three creep regimes has been obtained by introducing experimentally evaluated creep strengths and the so-called characteristic creep strain.

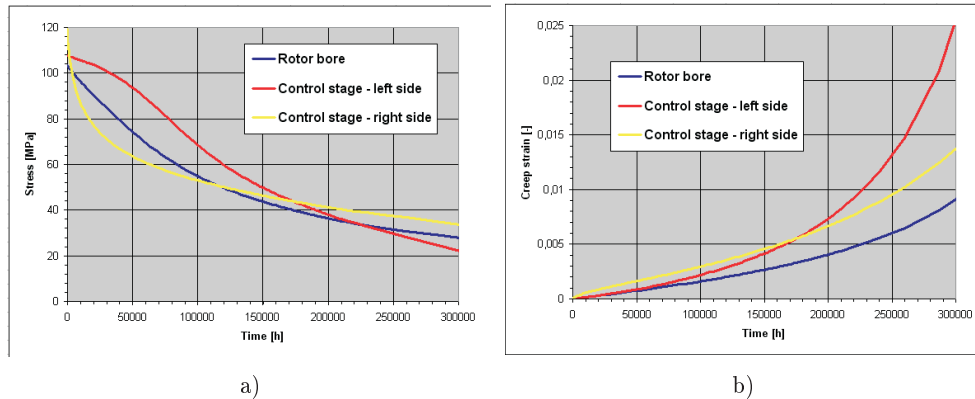


Figure 8. Huber-Mises equivalent stress relaxation (a) and creep strain accumulation (b) in the most highly efforted rotor locations.

The presented model correctly describes both creep curves at constant stress and temperature, and stress relaxation and creep strain accumulation in non-uniform temperature and stress fields, like those existing in turbine rotors. The presented results of numerical creep calculations were obtained for the first time for valve casing and turbine rotor of such a design. The valve casing was modelled as 3D component including specific design features not possible to be represented in 2D models used so far. For both components material and temperature specific creep data were employed in creep modelling, which ensured highly accurate predictions. The presented results of creep calculations of old components using the new mathematical model are in agreement with design calculations and operating experience. It justifies the use of this model to creep calculations of old Zamech turbines having specific design features and using different materials.

Acknowledgements Author would like to thank colleague from Engineering Department Mr Michał Osipiak, BEng, for preparing 3D model of the valve casing in CATIA v. 5 program.

Received in November 2012

References

- [1] Visvanathan R.: *Damage Mechanisms and Life Assessment of High-Temperature Components*. ASM Int., Metals Park, Ohio 1989.
- [2] Webster G.A., Ainsworth R.A.: *High Temperature Component Life Assessment*. Chapman & Hall, London 1994.

-
- [3] Bolton J.: *A 'characteristic-strain' model for creep*. In: Proc. ECCC/IMEchE Conf. on *Creep and Fracture in High Temperature Components* (J.A. Shibli, S.R. Holdsworth, G. Merckling, Eds.), London, Sept. 2005, 465–477.
 - [4] Norton F.H.: *The Creep of Steel at High Temperatures*. McGraw-Hill, London 1929.
 - [5] Chmielniak T., Kosman G., Rusin A.: *Creep of Thermal Turbines Components*. WNT, Warsaw 1990.
 - [6] Bolton J.: *Analysis of structures based on a characteristic-strain model of creep*. In: Proc. ECCC/IMEchE Conf. on *Creep and Fracture in High Temperature Components* (J.A. Shibli, S.R. Holdsworth, G. Merckling, Eds.), London, Sept. 2005, 1032–1045.
 - [7] ABAQUS User's Manual, Ver. 6.6, 2006.
 - [8] Zienkiewicz O.C., Taylor R.L., Zhu, J.Z.: *The Finite Element Method: Its Basis and Fundamentals*. Elsevier, 2006.
 - [9] Bartsch H.: *A new creep equation for ferritic and martensitic steels*. Steel Res. **66**(1995), 9, 384–388.
 - [10] Binda L., Holdsworth S.R., Mazza E.: *The exhaustion of creep ductility in 1CrMoV steel*. Int. J. Pres. Ves. Pip. **87**(2010), 6, 319–325.